

# Modeling and Active Vibration Control of a Smart Structure

Nader Ghareeb and Rüdiger Schmidt

*Institute of General Mechanics, RWTH Aachen University of Technology, Templergraben 64, Aachen, Germany*

**Keywords:** Super Element Model, Lyapunov Function Controller, Strain Rate Feedback Controller.

**Abstract:** Active vibration control of flexible structures has gained much attention in the last decades. The major components of any active vibration control system are the mechanical structure susceptible to vibration, sensor(s) to perceive it, actuator(s) to counteract the influence of disturbances causing vibration and finally, the controller responsible for the generation of appropriate control signals. In this paper, a Lyapunov function controller and a strain rate feedback controller (SRF) are used to attenuate the vibrations of a cantilevered smart beam excited by its first eigenmode. A super element (SE) with a finite number of degrees of freedom (DOF) is derived from the modified and damped finite element (FE) model. The state-space (SS) equations of the same model are also extracted. Controllers are applied to the SE and SS models and results are presented and compared.

## 1 INTRODUCTION

In modern engineering, weight optimization has always the highest priority during the design of structures. Despite all its advantages, it results in lower stiffness and less internal damping which cause the structure to become more sensitive to vibrations which could even lead to its failure (Ghareeb and Radovicic, 2009). One way to overcome this problem is to implement active or smart materials that can be controlled in accordance to the disturbances or oscillations sensed by the structure itself. The coupled electromechanical properties of smart materials, which are used here in the form of piezoelectric ceramics, make them well suited for the use as distributed sensors and actuators for controlling structural response. In the sensor application, mechanically induced deformations can be determined from measurement of the induced electrical potential, whereas in actuator applications deformation or strains can be controlled through the introduction of an appropriate electric potential (Narayanan and Balamurugan, 2003). Active vibration control has been applied at the beginning on ships (Mallock, 1905), and later on aircrafts (Hort, 1934). The rapid developments in this field lead after that to the use of point actuators and sensors to control flexible systems based on the knowledge of elastic mode frequencies and mode shapes at their location (Balas, 1978). The use of piezoelectric materials as actuators and sensors for noise and vibration control has been illus-

trated extensively over the past 30 years. An active vibration damper for a cantilever beam using a distributed parameter actuator was designed by (Bailey, 1984). Three different control algorithms to control the cantilevered beam vibration with piezoactuators were developed and implemented by (Bailey and Hubbard, 1985). A rigorous study on the stress-strain-voltage behavior of piezoelectric elements bonded to beams was presented by (Crawley and de Luis, 1987) and (Crawley and Anderson, 1990). Many other researchers have also investigated the implementation and use of piezoelectric actuators like (Fanson and Chen, 1986), (Preumont, 2002), etc.

The present work comprises modeling of a smart beam and the design of active linear controllers to control its vibrations. The piezoactuator is initially modeled and the relation between voltage and moments at its ends is examined. A modified FE model of the smart beam is then created. The damping coefficients are calculated and added to it prior to the reduction to a SE with a finite number of DOF. The SS model is also extracted to check the controllers. The FE- and SE models are validated by performing a modal analysis and comparing the results to the experimental ones. Finally, a Lyapunov function controller and a SRF controller are introduced and implemented on the SE and the SS models of the smart beam and results are shown. The FE package SAMCEF is used for the creation of the FE and the SE models, and MATLAB-SIMULINK is used for the implementation of the controllers in the SS form.

## 2 MODELING

The first step in designing a control system is to build a mathematical model of the system and disturbances causing the unwanted vibrations. The structural analytical model can be derived by using the FE method. The smart structure used here consists of a steel beam, a bonding layer and an actuator (Figure 1).

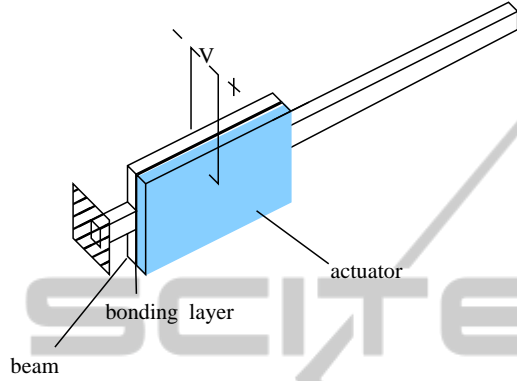


Figure 1: The smart beam.

### 2.1 Actuator Modeling

The introduction of an actuator implies the implementation of an appropriate electric potential to control the vibrations in the smart structure (converse piezoelectric effect). The voltage applied can be represented by two equal moments with opposite directions concentrated at its ends (Fanson and Chen, 1986). The behavior of the piezoelectric material is assumed to be linear throughout this work. By considering the schematic layout of the middle portion of the smart beam (Figure 2), if a voltage  $V$  is applied across the piezoelectric actuator while assuming one dimensional deformation, the piezo-electric strain  $\epsilon_p$  in the piezo is:

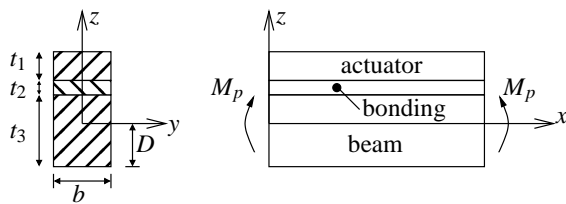


Figure 2: A schematic layout of the composite beam.

$$\epsilon_p = \frac{d_{31}}{t_1} \cdot V \quad (1)$$

$V$  is the voltage of the piezo-electric actuator,  $d_{31}$  the electric charge constant and  $t_1$  its thickness. The longitudinal stress can be expressed with Hooke's law as:

$$\sigma_p = E_1 \cdot \epsilon_p \quad (2)$$

where  $E_1$  is the Young's modulus of the piezo

This stress generates a bending moment  $M_p$  around the neutral axis of the composite beam given by:

$$M_p = \int_{(t_2+t_3-D)}^{(t_1+t_2+t_3-D)} \sigma_p \cdot b \cdot z dz \quad (3)$$

By considering the equilibrium of moments about the neutral axis:

$$\int_{beam} \sigma_3 dA + \int_{adhesive} \sigma_2 dA + \int_{piezo} \sigma_1 dA = 0 \quad (4)$$

the position of the neutral axis  $D$  is found.

Substituting  $D$ , (1) and (2) in (3) determines the bending moment generated by the piezo  $M_p$  as a function of the voltage  $V$ :

$$M_p = \frac{E_1 E_2 (t_1 t_2 + t_2^2) + E_1 E_3 (t_3^2 + t_1 t_3 + 2 t_2 t_3)}{2(E_1 t_1 + E_2 t_2 + E_3 t_3)} d_{31} b V$$

Now, the actuator moment can be taken instead of the voltage as input to the controllers that will be designed and implemented.

### 2.2 FE Modeling of the Smart Beam

The resultant FE model of the smart beam must be faithfully representative so that it can be used for further applications like control analysis (He and Fu, 2001). In order to find the best FE model, the optimal element type and size must be selected. Thus, a modal analysis of the real beam is experimentally performed and then the results are compared to those from the FE with different element types used. A detailed geometry of the smart beam is shown (Figure 3) and the material properties and thickness of each part are represented (Table 1).

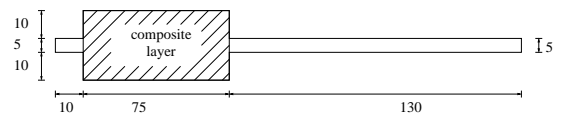


Figure 3: A detailed geometry of the smart beam [dimensions in mm].

Table 1: Parameters of the components of smart beam.

	Beam	Bonding	Actuator
Material	steel	epoxy	PIC 151
Thickness [mm]	0.5	0.036	0.25
Density [ $kg/m^3$ ]	7900	1180	7800
Young's mod. [GPa]	210	3.546	66.667

Table 2: Comparison between FE and SE models.

	FE model	Experiment
1 <sup>st</sup> eigenfrequency [Hz]	13.81	13.26
2 <sup>nd</sup> eigenfrequency [Hz]	42.67	41.14

**2.2.1 FE - Type and Size**

The smart beam is modeled as a composite shell with three layers, but without any relative slip among the contact surfaces. Hence, each layer has its own mechanical properties. To validate the element type used, a modal analysis is done and the first two eigenfrequencies are read and compared to those from the experiment (Table 2).

Although reducing the element size can improve the solution accuracy, but the use of excessively fine elements may result in unmanageable computations that exceed the memory capabilities of existing computers (Ko and Olona, 1987). The analysis shows that using an element size less than 1 mm doesn't make any significant change on the values of the 1<sup>st</sup> and 2<sup>nd</sup> eigenfrequencies of the smart beam.

**2.2.2 Damping Characteristics**

Damping parameters are of significant importance in determining the dynamic response of structures (Lee and Davidson, 2004). In this work, the damping is assumed to be viscous and frequency dependent for the sake of convenience and simplicity. A special case of viscous damping is known as the proportional or Rayleigh damping. The damping matrix is thus expressed as a linear combination of mass and stiffness matrices of the undamped model (Rayleigh, 1877):

$$C = \alpha M + \beta K \tag{5}$$

where  $\alpha$  and  $\beta$  are real scalars that need to be determined. To do that, many methods are available (Spears and Jensen, 2009) and (Adhikari, 2000). However, a method that was developed by (Chowdhury and Dasgupta, 2003) is used in this work.

**3 THE SUPER ELEMENT**

The main virtue of this technique is the ability to perform the analysis of a complete structure by using results of prior analysis of different regions comprising the whole structure. Thus, all DOF considered useless for the final solution will be condensed and the rest will be retained. This means, the DOF of the whole system will correspond to the retained nodes plus a number of internal deformation modes. To construct

the SE, the component-mode method is used (Craig and Bampton, 1968), (Rickelt-Rolf, 2009).

**3.1 The Component-mode Method**

also called method of Craig-Bampton, it implies that the basic substructure is split into a certain number of substructures. The DOF of each substructure are then classified into boundary DOF and internal DOF. The boundary DOF are shared by several substructures, while the internal DOF belong only to the considered substructure. The behavior of each substructure is described by the combination of two types of component modes; the constrained modes and the normal vibration modes. The former are determined by assigning a unit displacement to each boundary DOF while all other boundaries DOF are being fixed. The latter correspond to the vibration modes obtained by clamping the structure at its boundary. It is thus assumed that the behavior of the substructure in the global system can be represented by superimposing the constrained modes and a small number of normal modes. Hence, by retaining only the low-frequency vibration modes, the substructure's dynamic deformed shape is represented with sufficient accuracy.

**3.2 SE Modeling**

In order to construct a SE, the retained nodes and the condensed nodes must be designated and the number of internal modes to be used must be specified. The retained nodes are usually those where boundary conditions are applied, or where stresses, displacements,...etc are applied or measured. Based on the current work, 10 internal modes responding to about 95% participation of the mass are used and five retained nodes are considered (Figure 4). Node 1 is clamped, actuator moments are added on node 2 and node 3. Node 4 is used as a secondary sensor (for future works), and node 5 is used as a sensor to measure the tip displacement. A comparison between the FE and the SE models is shown in (Table 3) and (Table 4). Results of modal analyses on both models don't show a big difference concerning the eigenfrequencies.

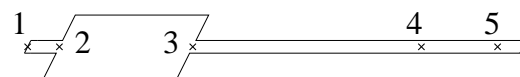


Figure 4: The retained nodes of the super element.

**4 THE STATE SPACE MODEL**

The fundamental equation describing the dynamic

Table 3: Characteristics of FE and SE models.

	FE model	SE model
Number of nodes	8206	5
Number of elements	2575	1
DOF	49236	34

Table 4: Comparison between the eigenfrequencies.

	FE model	SE model	% Error
1 <sup>st</sup> freq [Hz]	13.811	14.249	3.07
2 <sup>nd</sup> freq [Hz]	42.673	43.414	1.71

behavior of a damped structure discretized by the FE method is written in the form:

$$M\ddot{q}(t) + C\dot{q}(t) + Kq(t) = f(t) \quad (6)$$

where  $q(t)$  is the state vector which collects the displacements of the structure by DOF, and the  $f(t)$  vector expresses the applied loads. If the total number of DOF of the FE model is  $n$ , then the dimension of the state vector  $q(t)$  is also  $n$ , and that of the mass, stiffness and damping matrices will be  $n * n$ . However, since a SE is constructed and the desired results only concern specific locations of the structure,  $n$  will be reduced to  $s$ . In this case:

$$s = r + m - 6 \quad (7)$$

$r$  and  $m$  are the number of retained nodes, and the number of internal modes chosen.

The SS model is written according to (6) with dimensions of the SE model. The general form is:

$$\dot{x} = Ax + Bu, \text{ and } y = Cx + Du \quad (8)$$

$x$  is the state vector,  $u$  and  $y$  are the input and output vectors. By using a Fortran code, and upon specifying the type and position of inputs and outputs, the SS model of the SE model is created.

## 5 CONTROLLER DESIGN

The performance of smart structures for active vibration control depends strongly on the control algorithm accompanied with it. The objective is to design controllers capable of damping the vibrations due to the first eigenmode of the smart beam. The beam is initially excited with its first eigenmode and then it is left to vibrate freely. At this moment, the controllers are activated. Two vibration suppression methods are used; Lyapunov stability-based theorem control and the SRF control.

### 5.1 Lyapunov Stability Theorem

Although there is no general procedure for constructing a Lyapunov function, yet any function can be considered as a candidate if it meets some requirements, i.e. positive definite, equal to zero at the equilibrium state and with its derivative less or equal to zero (Khalil, 1996). Now, the energy equation of a thin Bernoulli-Euler beam modeled as a single FE in a one-dimensional system with length  $h$  and left point coordinate  $x_i$ , will be considered as a Lyapunov function candidate:

$$U = \frac{1}{2} \int_{x_i}^{x_i+h} \left[ \rho \left( \frac{\partial y}{\partial t} \right)^2 + EI \left( \frac{\partial^2 y}{\partial x^2} \right)^2 \right] dx \quad (9)$$

This function is locally positive definite, continuously differentiable and equal to zero at the equilibrium state. Yet, the derivative of this function must be smaller or less than zero.

$$\dot{U} = \int_{x_i}^{x_i+h} \left[ \rho \ddot{y} \dot{y} + EI \frac{\partial^2 y}{\partial x^2} \frac{\partial}{\partial t} \left( \frac{\partial^2 y}{\partial x^2} \right) \right] dx \quad (10)$$

Substituting the equations for the bending moment  $M$  and shear force  $V$  in a beam (Petyt, 2003) and assuming there is no shear yields:

$$\dot{U} = M \left( \dot{y}'_{x_i+h} - \dot{y}'_{x_i} \right) \quad (11)$$

To ensure that (11) is always smaller or equal to zero, the actuator moment  $M$  can have the value:

$$M = -k \left( \dot{y}'_{x_i+h} - \dot{y}'_{x_i} \right) \quad (12)$$

where  $k$  is a positive constant. Substituting (12) in (11) yields:

$$\dot{U} = -k \left( \dot{y}'_{x_i+h} - \dot{y}'_{x_i} \right)^2 \leq 0 \quad (13)$$

In this case, (12) can be used as the controller for the smart beam.

#### 5.1.1 SE Model with Controller

Based on the SE model created, two equal moments at nodes 2 and 3 (but with opposite directions) are added, where each one of them is a function of the velocities at both nodes according to (12). The effectiveness of this control strategy is shown in (Figure 5), and its effect on the magnitude of the eigenmode on the FFT spectrum diagram is illustrated in (Figure 6).

#### 5.1.2 SS Model with Controller

In the SS, two steps are done. In step one, the only input is the forced excitation with the first eigenmode

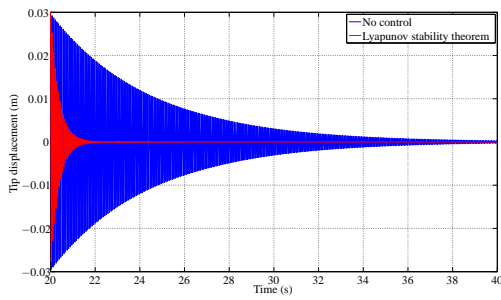


Figure 5: Tip displacement vs. time with and without controller during the free vibration (SE model is used).

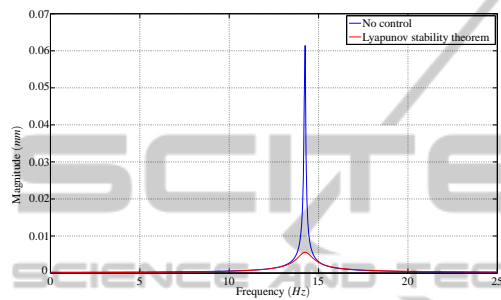


Figure 6: The FFT spectrum of the smart beam.

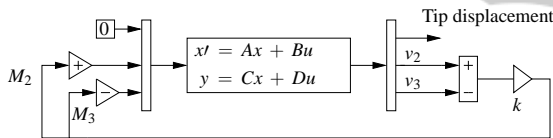


Figure 7: The SS model of the smart beam with controller.

and the output consists of the state vectors that are fed as initial conditions for the second step. In step two, (Figure 7), the input consists of both actuator moments. The output comprises the tip displacement at the 5<sup>th</sup> retained node, and the velocities at the 2<sup>nd</sup> node and 3<sup>rd</sup> node. Based on the Lyapunov stability theorem, the output multiplied by a constant  $k$  is fed back as actuator moments with different signs.

### 5.1.3 Comparison of Results from Both Models

The controller is implemented on both models and a very slight difference is seen if the output curves are zoomed (Figure 8). This is due to the fact that different time steps are used in both models. Thus, using a SE model decreases the simulation time and can show more results (e.g. stresses, energy curves, etc).

## 5.2 Strain Rate Feedback Control

The SRF control can be used for active damping of a flexible space structure (Fei and Fang, 2006). The

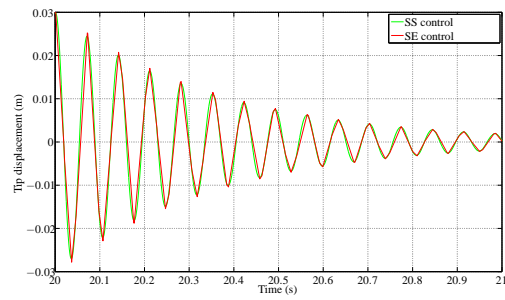


Figure 8: Tip displacement vs. time with both models.

structural velocity coordinate is fed back to the compensator, and the compensator position coordinate multiplied by a negative gain is fed back to the structure. The SRF model can be presented with the following equations:

$$\ddot{\xi} + 2\zeta\dot{\xi} + \omega^2\xi = -G\omega^2\eta \quad (14)$$

$$\ddot{\eta} + 2\zeta_c\omega_c\dot{\eta} + \omega_c^2\eta = \omega_c^2\dot{\xi} \quad (15)$$

$\xi$  is the modal coordinate of structure displacement,  $\zeta$  is the damping ratio of the structure,  $\omega$  is its natural frequency,  $G$  is the feedback gain,  $\eta$  is the compensator coordinate,  $\zeta_c$  is the damping ratio of the compensator and  $\omega_c$  its natural frequency.

Since all the parts of the smart beam are integrated in a single SE, it is supposed that the smart beam and the controller have the same damping ratio and the same eigenfrequency. Applying this assumption in the equation of the smart beam gives:

$$\ddot{\xi} + 2\zeta\omega\dot{\xi} + (\omega^2 + G\beta\omega^2)\xi = 0 \quad (16)$$

In this case, there will be an increase in the stiffness of the structure (active stiffness). However, the stability condition is not clearly defined here due to the fact that the closed-loop damping and stiffness matrices of the whole system cannot be symmetrized (Newman, 1992). The effectiveness of the SRF controller is shown in (Figure 9). The magnitude of the eigenmode of the system decreases as well (Figure 10).

## 6 CONCLUSIONS AND FUTURE WORK

In this work, the basic procedures for the modeling and simulation of a smart beam were presented and the SE and SS models were derived. A Lyapunov function and a SRF controllers were designed and implemented, and their effectiveness was checked.

In the future, an observer will be designed to count for the geometrical nonlinearities which were not considered in this work. Nevertheless, more eigenmodes



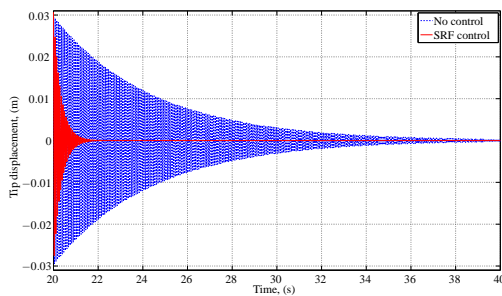


Figure 9: Tip displacement vs. time with the SRF controller.

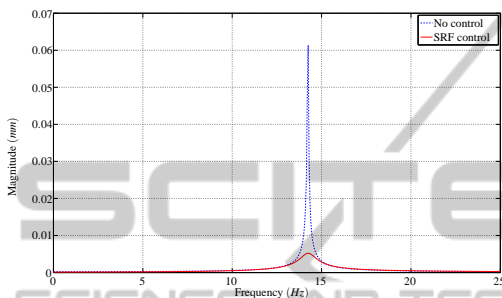


Figure 10: The FFT spectrum of the smart beam.

will be controlled, and other control strategies (e.g. positive position feedback, PID controllers...etc) will be investigated and implemented.

## REFERENCES

- Adhikari, S. (2000). *Damping Models for Structural Vibrations*. PhD thesis, Cambridge University.
- Bailey, T. (1984). Distributed-parameter vibration control of a cantilever beam using a distributed-parameter actuator. Master's thesis, Massachusetts Institute of Technology.
- Bailey, T. and Hubbard, J. (1985). Distributed piezoelectric-polymer active vibration control of a cantilever beam. *AIAA Journal of Guidance and Control*, 6:605–611.
- Balas, M. (1978). Active control of flexible systems. *Journal of Optimization Theory and Applications*, 25:415–436.
- Chowdhury, I. and Dasgupta, S. (2003). Computation of rayleigh damping coefficients for large systems.
- Craig, R. and Bampton, M. (1968). Coupling of substructures for dynamic analysis. *AIAA Journal*, 6:1313–1319.
- Crawley, E. and Anderson, E. (1990). Detailed models of piezoceramic actuation of beams. *Journal of Intelligent Material Systems and Structures*, 1:4–24.
- Crawley, E. and de Luis, J. (1987). Use of piezoelectric actuators as elements of intelligent structures. *AIAA Journal*, 25:1373–1385.
- Fanson, J. and Chen, J., editors (1986). *Structural Control by the use of Piezoelectric Active Members*, volume 2 of *Proceedings of NASA/DOD Control-Structures Interaction Conference*. NASA. CP-2447.
- Fei, J. and Fang, Y., editors (2006). *Active Feedback Vibration Suppression of a Flexible Steel Cantilever Beam Using Smart Materials*. Proceedings of the First International Conference on Innovative Computing, Information and Control (ICICIC'06).
- Ghareeb, N. and Radovic, Y. (2009). Fatigue analysis of a wind turbine power train. *DEWI Magazin*, 35:12–16.
- He, J. and Fu, Z. (2001). *Modal Analysis*. Butterworth-Heinemann.
- Hort, H. (1934). Beschreibung und versuchsergebnisse ausgeführter schiffsstabilisierungsanlagen. *Jahrb. Schiffbautechnik Ges.*, 35:292–312.
- Khalil, H. (1996). *Nonlinear Systems*. Prentice Hall, Madison.
- Ko, W. and Olona, T. (1987). Effect of element size on the solution accuracies of finite-element heat transfer and thermal stress analysis of space shuttle orbiter. Technical Memorandum 88292, NASA.
- Lee, J. B. J. and Davidson, B. (2004). Experimental determination of modal damping from full scale testing. In *13th World Conference on Earthquake Engineering*, number 310, Vancouver, Canada.
- Mallock, A. (1905). A method of preventing vibration in certain classes of steamships. *Trans. Inst. Naval Architects*, 47:227–230.
- Narayanan, S. and Balamurugan, V. (2003). Finite element modelling of piezolaminated smart structures for active vibration control with distributed sensors and actuators. *Journal of Sound and Vibration*, 262:529–562.
- Newman, S. (1992). Active damping control of a flexible space structure using piezoelectric sensors and actuators. Master's thesis, U.S. Naval Postgraduate School, California.
- Petyt, M. (2003). *Introduction to Finite Element Vibration Analysis*. Cambridge University Press.
- Preumont, A. (2002). *Vibration Control of Active Structures, An Introduction*. Kluwer Academic Publishers.
- Rayleigh, L. (1877). *Theory of Sound*, volume 1, 2. Dover Publications, New York.
- Rickelt-Rolf, C. (2009). *Modellreduktion und Substrukturtechnik zur effizienten Simulation dynamischer teilgeschädigter Systeme*. PhD thesis, TU Carolo-Wilhelmina zu Braunschweig, Germany.
- Spears, R. and Jensen, S., editors (2009). *Approach for Selection of Rayleigh Damping Parameters Used for Time History Analysis*, Proceedings of PVP2009, ASME Vessels and Piping Division Conference, Prague, Czech Republic.